www.vbripress.com/aml, DOI: 10.5185/amlett.2016.6111 Published online by the VBRI Press in 2016

Optical modes of vibration in a metamaterial slab including effects of retardation

G. Becerra O.[1*], J. C. Granada E.[2]

[1]*Programa de Ingeniería Electrónica, Facultad de Ingenierías, Universidad San Buenaventura Cali, La Umbría- Vía Pance, Cali, 25162, Colombia*
[2]*Departamento de Física, Universidad del Valle, Calle 13#100-00, Cali 25162, Colombia*

[*]Corresponding author. Tel: (+57) 2488-2222; E-mail: gbecerra@usbcali.edu.co

Received: 25 August 2015, Revised: 22 November 2015 and Accepted: 26 March 2016

ABSTRACT

The frequencies of optical modes of vibration in a metamaterial slab, contacting with vacuum, are investigated when the slab dielectric permittivity and the magnetic permeability show resonant behavior. Retardation effects are included in the no radiative zone. On the basis of the linear response theory, we calculate the components of the electromagnetic Green propagator. The dispersion curves and the corresponding power spectra are determined from the poles and the imaginary part of these components. Two sets of surface polaritonic frequencies are found for transversal electric *TE*- and transversal magnetic *TM* surface modes, corresponding to bonding and antibonding oscillations of the electric and magnetic fields at the slab surfaces. It is shown that for all the range of values in the relation between the resonance frequency of magnetic permeability and the resonance frequency of the dielectric permittivity there is one *TE* and one *TM* backward mode with negative group velocities. This parameter relation determines if the frequency range of *TM* modes can be separated from the corresponding interval for *TE* modes. Present work can be extended to consider waves in photonic crystals containing anisotropic slabs with resonant behavior in the optical properties, which can be useful to design omnidirectional optical filters. Copyright © 2016 VBRI Press.

Keywords: Metamaterials; surface modes; polaritons.

Introduction

The study of electromagnetic waves in metamaterials and nanostructures has been the subject of considerable interest due to their unusual electromagnetic properties [**1-4**] which can be beneficial to design devices with unprecedented properties in imaging [**5**], sensing [**6-8**], ultrasound detection [**9**] or enhanced energy harvesting [**10**]. In systems containing metamaterials with frequency dependence in their dielectric permittivity ε and magnetic permeability μ, light interacts with a resonant medium by forming polaritonic waves (mixed excitations of the electromagnetic field with quasiparticles related to material resonances). The behavior of such excitations is governed by the dispersion determined by the material resonances. In particular, the presence of metamaterials in photonic crystals has implications for the existence of non-Bragg gaps in one dimensional [**11**] and two-dimensional structures [**12**]. In this sense, negative refraction of surface plasmon polariton and the existence of backward waves, with negative group velocity are of considerable interest [**13-15**].

Most of the papers on modes in systems containing metamaterials consider non-resonance behavior of the dielectric permittivity ε and the magnetic permeability μ [**16-20**]. The discussion of frequency regions far from the resonances of the refraction index allows neglecting the frequency dependence of the optical characteristics. In a recent report [**21**] it was shown that the simultaneous presence of resonances in the dielectric permittivity and the magnetic permeability can lead to the simultaneous existence of omnidirectional non-Bragg gaps for both transversal electric (TE) and transversal magnetic (TM) polarizations, which are robust to uniaxial anisotropic effects.

For this reason in the present communication we pay special attention to the region close to the resonance frequency of the magnetic permeability. For this purpose, we develop green function formalism in order to describe the power spectra and the dispersion relations of the surface modes in a metamaterial slab, which is bounded by lossless homogeneous dielectrics.

The work is organized as follows. The considered model and the general relations of the green function formalism are introduced in section 2. The dispersion curves of the transversal electric (*TE*) and the transversal magnetic (*TM*) modes are discussed in section 3 for frequencies close to the resonance frequency of the magnetic permeability; the power spectra of *TM* modes are also considered in this section. The results are summarized in section 4, with a brief indication to future perspectives.

Model and general relation

Description of the system

We consider a homogeneous and isotropic planar metamaterial formed by a slab of thickness l, which occupies the region $-l/2<z<l/2$. It is assumed that the

frequency dependencies of the dielectric permittivity and the magnetic permeability have resonant character and are chosen in the form

$$\varepsilon^{(2)}(\omega) = \varepsilon_{\infty} \frac{\omega^2 - \omega_{LO}^2}{\omega^2 - \omega_{TO}^2 + i\,\omega\,\Gamma_e},$$

$$\mu^{(2)}(\omega) = 1 - \frac{B\,\omega^2}{\omega^2 - \omega_m^2 + i\,\omega\,\Gamma_m},$$

where, ε_{∞} is the dielectric permittivity at high frequencies, ω_{LO} is the frequency associated with the electric plasmon mode, ω_{TO} (ω_m) is the resonant frequency of the dielectric permittivity (magnetic permeability), respectively; Γ_e and Γ_m are the damping constants in the active metamaterial medium and *B* is the filling factor. The regions $z < -l/2$, $z > l/2$ are occupied by lossless dielectric media 1, 3 with dielectric permittivities ε_1, ε_3, and magnetic permeabilities μ_1, μ_3 respectively.

Green's function formalism

By following the methodology described in [**22**], and used in [**23**] for the description of Tamm states at the interface between a conventional material and a one dimensional photonic crystal with metamaterials, the photon Green's tensor $D_{\mu\nu}(\boldsymbol{x}, \boldsymbol{x}'; \omega)$ is the solution of the equation

$$\left(\varepsilon(z;\omega)\mu(z;\omega)\frac{\omega^2}{c^2}\delta_{\lambda\mu} - \frac{\partial^2}{\partial x_\lambda \partial x_\mu} + \delta_{\lambda\mu}\nabla^2\right) D_{\mu\nu}(x, x'; \omega) = 4\pi\delta_{\lambda\nu}\delta(x - x') \quad (1)$$

where, $\mu, \nu = x, y, z$,

$\boldsymbol{x} = (\boldsymbol{x}_{//}, z)$,

$f(z;\omega) = f_1\theta(l/2 - z) + f_3\theta(z - l/2) + f_2\theta(l/2 - z)\theta(z - l/2)$, $f = \varepsilon, \mu$, $\theta(x)$ is the step function. At the boundaries the magnitudes $D_{i\nu}(\boldsymbol{x}, \boldsymbol{x}'; \omega)$, $\varepsilon_{z\mu} D_{\mu\nu}(\boldsymbol{x}, \boldsymbol{x}'; \omega)$, $\varepsilon_{i\lambda\mu} \frac{\partial}{\partial x_\lambda} D_{\mu\nu}(\boldsymbol{x}, \boldsymbol{x}'; \omega)$, $\varepsilon_{z\lambda\mu} \frac{\partial}{\partial x_\lambda} \mu_{\mu\nu} D_{\nu\sigma}(\boldsymbol{x}, \boldsymbol{x}'; \omega)$ must be continuous (i=x,y). The homogeneity in the *x*, *y* plane allows introducing the Fourier transformation

$$D_{\mu\nu}(\boldsymbol{x}, \boldsymbol{x}'; \omega) = \int \frac{d^2 k_{//}}{(2\pi)^2} \exp\left[i\boldsymbol{k}_{//} \bullet (\boldsymbol{x}_{//} - \boldsymbol{x}'_{//})\right] d_{\mu\nu}(\boldsymbol{k}_{//}, \omega; z, z')$$

and the isotropy in the *x*, *y* plane can be accounted by introducing the tensor $g_{\mu\nu}(\boldsymbol{k}_{//}, \omega; z, z') = S_{\mu\rho} S_{\sigma\nu} d_{\rho\sigma}(\boldsymbol{k}_{//}, \omega; z, z')$ where $S_{xx} = S_{yy} = \frac{k_x}{k_{//}}$, $S_{iz} = \delta_{iz}$. After a straightforward calculation, the following expressions for the diagonal components of the photon Green's tensor are obtained for the case $z' > 0$:

$$\frac{1}{4\pi} g_{xx}^{>}(z) = \frac{1}{2}\frac{c^2 k_0}{\omega^2}\frac{1}{\varepsilon_0}\left[\frac{f_p^-}{f_p^+}\exp[-k_0(z + z')] + \exp(-k_0|z - z'|)\right] \quad (2)$$

$$\frac{1}{4\pi} g_{yy}^{>}(z) = \frac{1}{2}\frac{1}{k_0}\left[\frac{f_s^-}{f_s^+}\exp[-k_0(z + z')] + \exp(-k_0|z - z'|)\right] \quad (3)$$

$$\frac{1}{4\pi} g_{zz}^{>}(z) = \frac{1}{2}\frac{c^2}{\omega^2}\frac{k_{//}^2}{k_0}\frac{1}{\varepsilon_0}\left[\frac{f_p^-}{f_p^+}\exp[-k_0(z + z')] - \exp[-k|z - z'|]\right] - \frac{1}{k^2}\delta(z - z') \quad (4)$$

$$f_r^{\pm} = \left(\frac{g_{r,1}}{k_z^{(1)}} - \frac{g_{r,2}}{k_z^{(2)}}\right)\left(\frac{g_{r,3}}{k_z^{(3)}} + \frac{g_{r,2}}{k_z^{(2)}}\right)\frac{1}{f^2} \mp \left(\frac{g_{r,1}}{k_z^{(1)}} + \frac{g_{r,2}}{k_z^{(2)}}\right)\left(\frac{g_{r,3}}{k_z^{(3)}} - \frac{g_{r,2}}{k_z^{(2)}}\right) f^2 \quad (5)$$

$$f = \exp\left(i k_z^{(2)} \frac{l}{2}\right),\ k_z^{(i)} = \sqrt{\frac{\omega^2}{c^2}\varepsilon^{(i)}\mu^{(i)} - k_x^2},$$

$$g_{r,i} = \varepsilon_i\,\delta_{pr} + \mu_i\,\delta_{sr}, \quad r = s, p, \quad i = 1,2,3$$

The poles of the Green tensor corresponding to $f_p^+ = 0$ give the dispersion relations of the *TM* modes arising in the considered system, whereas the dispersion relations of the *TE* modes correspond to the solutions of $f_s^+ = 0$. If the relations $k_x^2 \geq \frac{\omega^2}{c^2}\varepsilon^{(i)}\mu^{(i)}$ (i =1, 2, 3) take place, the modes exist in the nonradiative region of spectra. From the expressions for the diagonal Fourier components of the photon propagator of the considered system it is possible to obtain the peaks corresponding to the power spectra $\mathrm{Im}\sum_i |g_{ii}|$ of such modes. For the case $l \to \infty$, $\mu^{(i)} = 1$ expressions (2-5) reduce to those reported in the appendix of [**24**].

Results and discussion

In the following we introduce the dimensionless quantities ω/ω_{TO}, ck_x/ω_{TO} and the set of values $\varepsilon_{\infty} = 2$, $\omega_{LO} = 1.5\omega_{TO}$, $\frac{\omega_{TO} l}{c} = 0.1$, B=0.5, $\varepsilon_1 = \varepsilon_3 = 1$, $\mu_1 = \mu_3 = 1$, Γ_e=$10^{-3}\omega_{TO}$, Γ_m=$10^{-4}\omega_{TO}$, is used. The modes arising in the frequency range $0 < \omega < \max\{\omega_{LO}, \omega_m\}$ for different values of the resonance frequency ω_m will be considered.

Fig. 1(a) shows the surface polariton dispersion curves for a slab of metamaterial with resonance frequency $\omega_m = 0.5\omega_{TO}$. The dashed areas correspond to the existence of the metamaterial bulk modes. For these parameters the surface modes exist in the frequency intervals $\omega_m < \omega < \omega^*$ (for the *TE* modes) and $\omega_{TO} < \omega < \omega_{LO}$ (for the *TM* modes), where (ω^*/c, ω^*) corresponds to the transparency point in the plane (k_x, ω) where the dispersion curves of bulk modes intersect (i.e.,

$\varepsilon^{(2)}(\omega^*)\mu^{(2)}(\omega^*)=1$). The low frequency *TE* mode arises from the antibonding combination of the electric fields at the slab surfaces, it starts at the point where the resonance frequency ω_m intersects the line $\omega=ck_x$, then it increases with the in-plane wave vector k_x and in the nonretarded region of the spectra ($k_x>>\omega/c$), it tends to the frequency ω_{sm}, corresponding to the root of the relation $\mu^{(2)}(\omega_{sm})=-1$. On the other hand, the high frequency *TE* mode arises from the bonding combination of the electric fields at the slab surfaces, it starts at the transparency point (ω^*/c, ω^*), then it decreases with k_x and in the nonretarded region of the spectra ($\omega<<ck_x$), it tends to ω_{sm} for the whole interval of k_x where this mode exists, it is a backward wave.

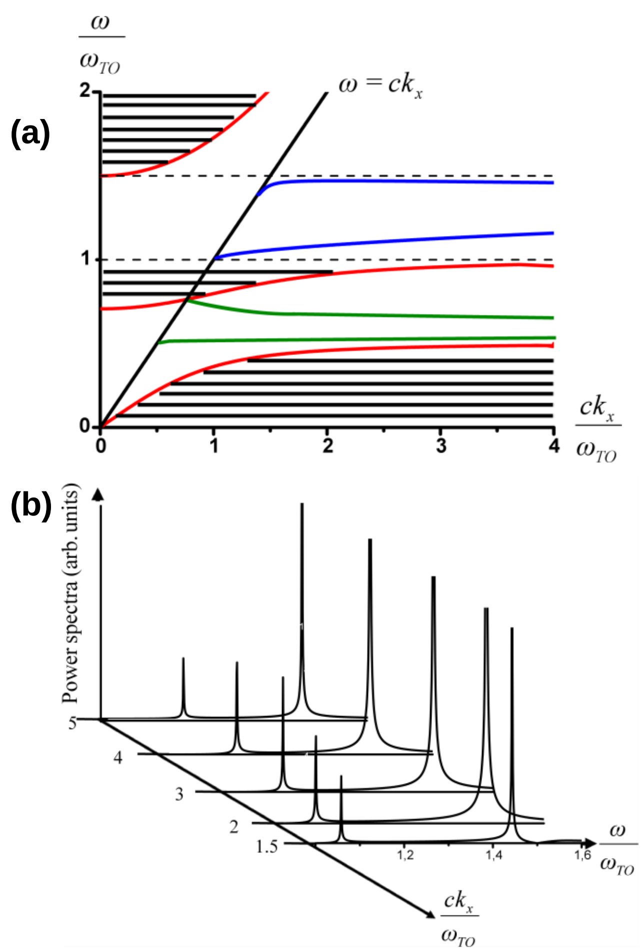

Fig. 1. Dispersion curves of surface polaritons *(a)* and power spectra of *TM* waves *(b)* arising in a slab of metamaterial for the parameter set $\varepsilon_\infty=2$, $\frac{\omega_{LO}}{\omega_{TO}}=1.5$, $\frac{\omega_{TO}l}{c}=0.1$, B=0.5, $\varepsilon_1=1$, $\mu_1=1$, $\frac{\omega_m}{\omega_{TO}}=0.5$. The regions of existence of bulk modes of medium 2 are shown with shade. Green (blue) lines correspond to *TE* (*TM*) modes.

The frequency range of *TM* is separated from the corresponding interval for *TE* modes by the interval $\omega^*<\omega<\omega_{TO}$. As in the case of *TE* modes, the low (high) frequency *TM* mode arises from the antibonding (bonding) combination of the magnetic fields at the slab surfaces; the corresponding dispersion curves start at the point where the resonance frequency ω_{TO} intersects the line $\omega=ck_x$ and in the nonretarded region of the spectra both dispersion curves tend to the frequency ω_{se}, corresponding to the root of the relation $\varepsilon^{(2)}(\omega_{se}) = -1$. The antibonding *TM* mode is a forward wave in the whole interval of k_x where this mode exists, whereas the bonding *TM* is a forward wave only in the interval of k_x where retarded effects are relevant. In the nonretarded region of the spectra the bonding *TM* mode is a backward wave.

In **Fig. 1**(b) we show the power spectra of the *TM* modes for different values of the in-plane wave vector k_x. Note that for $k_x>\omega_{LO}/c$ there are two peaks corresponding to two localized *TM* modes with frequencies above the resonance frequency ω_{TO} but for $k_x<\omega_{LO}/c$ there is only one peak corresponding to the antibonding *TM* wave. Note also that the position of the peaks corresponding to the mode closest to ω_{TO} is an increasing function of the in-plane wave vector, whereas for the bonding *TM* mode the frequency at the maxima of such peaks slowly decreases with k_x.

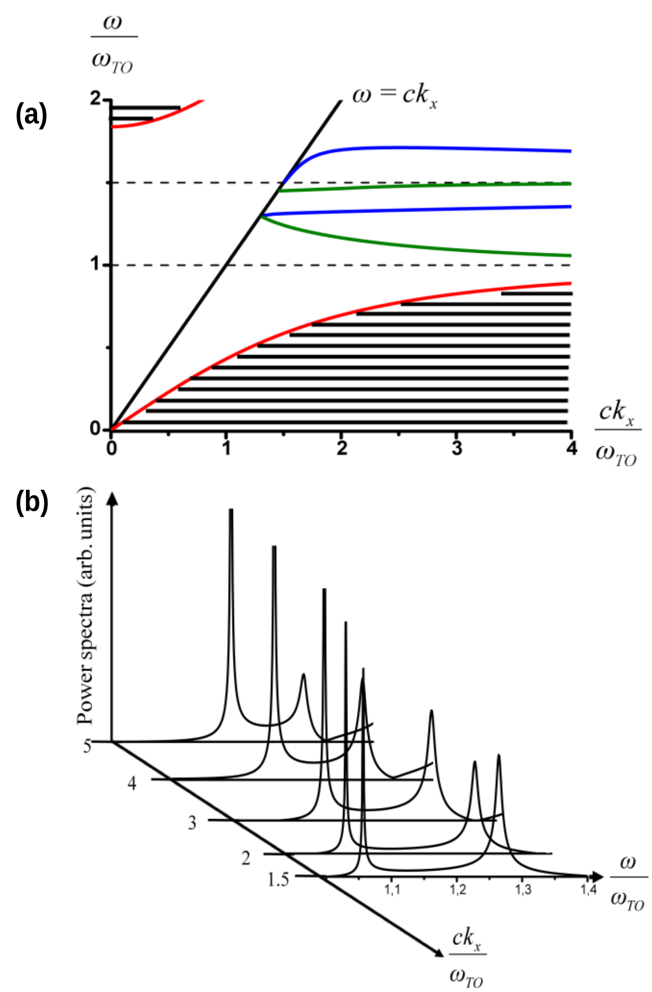

Fig. 2. Same as in **Fig. 1**, but for $\omega_m=1.3\omega_{TO}$.

Fig. 2 shows the dispersion curves and the power spectra of surface polaritons arising in a slab of metamaterial for the case when the resonance frequency belongs to the interval $\omega_{TO}<\omega_m<\omega_{LO}$. In this case the frequency ranges for existence of *TE* and *TM* modes are not separated by a frequency interval, in contrast to the case $\omega_m < \omega_{TO}$. Retarded effects are relevant for the bounding *TM* modes and can be neglected for $k_x \gg \omega_{LO}/c$; under such condition this mode is a backward wave. Note also that the antibounding *TE* mode and the antibonding *TM* modes start at the same point, being the latest mode a backward wave with a frequency asymptotically approaching ω_{sm}. This result is in agreement with that reported for surface polaritons of a semi-infinite metamaterial medium [**25-27**].

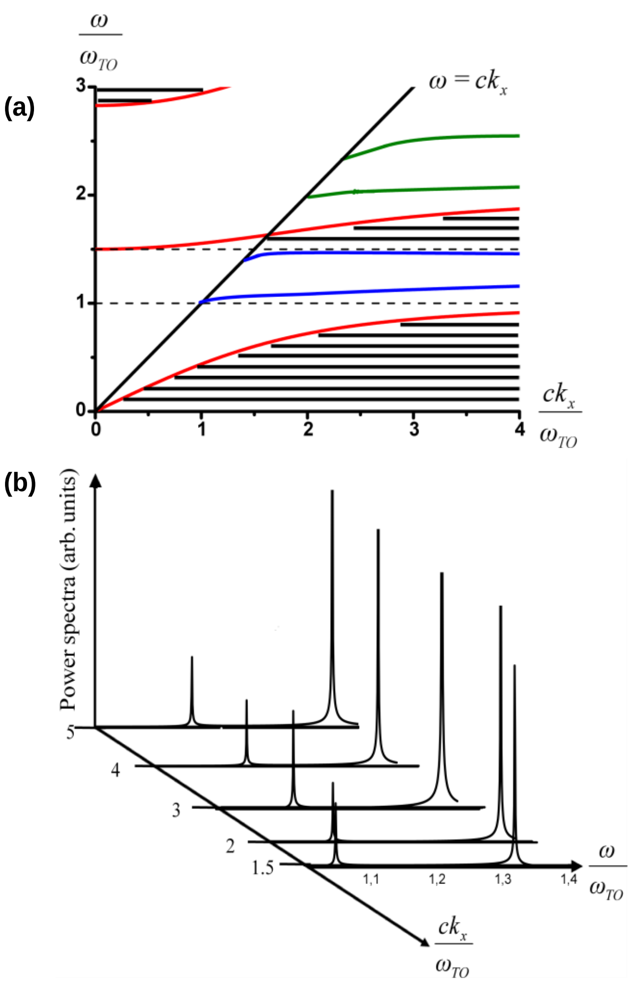

Fig. 3. Same as in **Fig. 1**, but for $\omega_m = 2\,\omega_{TO}$.

In **Fig. 3** the case $\omega_m > \omega_{LO}$ is considered. Note that the set of *TE* dispersion curves is above the corresponding set of *TM* curves and the frequency range for the existence of *TM* is separated from the corresponding interval for *TE* modes by the interval $\omega_{LO} < \omega < \omega_m$. Retarded effects are relevant for the bounding *TE* modes and can be neglected for $k_x \gg \omega_{sm}/c$. On the other hand, these effects can be neglected for both *TM* modes for $k_x \gg \omega_{LO}/c$. From the positions of the peaks of the power spectra of *TM* waves arising.in the considered slab of metamaterial we can see that mode closest to ω_{TO} is an increasing function of the in-plane wave vector, whereas for the bonding *TM* mode the frequency at the maxima of such peaks slowly decreases with k_x. This behavior is qualitatively similar to the behavior of *TM* modes when the resonance frequency ω_m is below ω_{TO}.

Conclusion

The electromagnetic propagator was calculated in order to describe the properties of *TE*- and *TM* surface modes arising on the interface between conventional and metamaterial media with a dielectric permittivity and a magnetic permeability showing resonant character and paying special attention to the character of the modes for different relations between the resonant frequency ω_m of the magnetic permeability and the resonant frequency ω_{TO} of the dielectric permittivity. Two sets of surface polaritonic frequencies are found for *TE*- and *TM* surface modes, corresponding to bonding and antibonding oscillations of the corresponding electric and magnetic fields at the slab surfaces. It was shown that for all the range of values in the relation ω_m/ω_{TO} there is one *TE* and one *TM* backward mode with negative group velocities. On the other hand, if the resonance frequency ω_m is lower than ω_{TO} or higher than the frequency associated with the electric plasmon mode ω_{LO}, the frequency range of TM is separated from the corresponding interval for TE modes and for resonance frequencies $\omega_{TO} < \omega_m < \omega_{LO}$ such frequency intervals are not separated.

This work can be extended to consider propagation of electromagnetic waves in photonic crystals containing slabs with resonant behavior in the dielectric permittivity and the magnetic permeability. Additionally, anisotropic systems with strong dependence of frequency of the dielectric permittivity and the magnetic permeability tensors can be considered. These perspectives could be useful for the future design of omnidirectional, robust to polarization, optical filters because the incorporation of thin films made of an active medium, positioned adjacent to the core layer of a waveguide with negative refractive index, can completely eliminate the dissipative losses under a slow or detained regime, where the effective index of the guided light wave remains negative.

Acknowledgements

This work is part of the research project "Wave propagation in two dimensional photonic crystals composed of single-negative metamaterials with mixed shapes and rods", supported by Universidad San Buenaventura-Cali. JCG thanks the Excellence Center of New Materials (CENM) for financial support of the research group.

Author contributions

Both authors conceived the plan, performed the analitical and numerical calculations and wrote the paper. Authors have no competing financial interests.

Reference

1. Markoš, P.; Soukoulis, C. M.; Wave Propagation: From Electrons to Photonic Crystals and Left-Handed Materials, Princeton University, USA **2008**.
ISBN: 9781400835676
2. Ramakrishna, S.; Grzegorczyk T.; Physics and Applications of Negative Refractive Index Materials, Taylor and Francis Group, USA, **2009.**
ISBN: 9781420068757

3. Vasilantonakis, N; Nasir, M.; Dickson, W.; Wurtz,G.; Zayats, A.; *Laser & Photonics Reviews*, **2015**, *9*, 345.
   DOI: 10.1002/lpor.201400457
4. Corbitt, S. J.; Francoeur, M.; Raeymaekers, B.; *Journal of Quantitative Spectroscopy and Radiative Transfer*, **2015,** *158*, 3.
   DOI: 10.1016/j.jqsrt.2014.12.009
5. Kim, M.and Rho, J.; *Nanoconvergence* , **2015**, *2*, 22.
   DOI: 10.1186/s40580-015-0053-7
6. Ding, C.; Jiang, L.; Wu, L.; Gao R.; Xu, D.; Zhang, G.; Yao, J.; *Optics Communications*, **2015**, *350*, 103.
   DOI: 10.1016/j.optcom.2015.03.062
7. Nasir, M.; Dickson, W.; Wurtz, G.; Wardley, W.; Zayats, A.; *Adv. Mater*, **2014**, *26*, 3532.
   DOI: 10.1002/adma.201305958
8. Wan, M.; Yuan, S., Dai K.; Song, Y.; Zhou, F.; *Optik - International Journal for Light and Electron Optics*, **2015**, *126*, 541.
   DOI: 10.1016/j.ijleo.2015.01.006
9. Yakovlev, V.; Dickson, W.; Murphy, A.; McPhillips, J.; Pollard, R.; Podolskiy, V.; Zayats, A.; *Adv. Mater*, **2013**, *25*, 2351.
   DOI: 10.1002/adma.201300314
10. Chen, Z., Guo, B., Yang, Y., Cheng, C., *Physica B* **2014**, *438*, 1.
    DOI: 10.1016/j.physb.2013.12.040
11. Reyes-Gómez, E.;.Cavalcanti, S; Oliveira, L.; *Superlattices and Microstructures*, **2013**, *64*, 590.
    DOI: 10.1016/j.spmi.2013.10.029
12. Mejía-Salazar, J.; Porras-Montenegro, N.; *Superlattices and Microstructures*, **2015**, *80*, 118.
    DOI: 10.1016/j.spmi.2015.01.002
13. Sharma, D., Verma, A., Prajapati, Y. K.; Singh, V. and Saini, J. P.; *Optical and Quantum Electronics* **2013**, *45*, 105
    DOI: 10.1007/s11082-012-9607-7
14. Chiadini, F.; Fiumara, V.; Scaglione, A.; Lakhtakia, A.; *Optics Communications,* **2016**, *363*, 201.
    DOI: 10.1016/j.optcom.2015.11.031
15. Shportko, K.; Barlas, T.; Venger, E.; El-Nasser, H.; Ponomarenko, V.; *Current Applied Physics*, **2016**, *16*, 8.
    DOI: 10.1016/j.cap.2015.10.001
16. Rahimi, H., *Physica B* **2014**, *433*, 1.
    DOI: 10.1016/j.physb.2013.10.011
17. Ru, Wua M.; Jang, Wub C.; Jinn Chang, S.; *Physica E* **2014**, *64*, 146.
    DOI: 10.1016/j.physe.2014.07.023
18. Barati, M.; Aghajamali A.; *Physica E* **2016**, *79*, 20.
    DOI: 10.1016/j.physe.2015.12.012
19. Gómez-Urrea, H.A., Duque, C.A. , Mora-Ramos, M.E., *Superlattices and Microstructures* **2015**, *87*, 115.
    DOI: 10.1016/j.spmi.2015.05.043
20. Reyes-Gómez, E.; Cavalcanti, S. B.; Oliveira L.E.; *Superlattices and Microstructures* **2013**, *64*, 590.
    DOI: 10.1016/j.spmi.2013.10.029
21. Moncada-Villa, E.; Mejía-Salazar, J.; Granada, J.; *Optics Letters* **2015**, *40*, 10.
    DOI: 10.1364/OL.40.002345
22. G.Orozco ,; J. Granada,; *Microelectronics Journal* **2008**, *39*, 1268 .
    DOI: 10.1016/j.mejo.2008.01.012
23. Becerra, G.; Granada, J.; *Physica B* **2014**,45589.
    DOI: 10.1016/j.physb.2014.07.053
24. Maradudin, A.; Mills, D.; *Physical Review B*, **1975**, *11*, 1392.
    DOI: 10.1103/PhysRevB.11.1392
25. Ruppin, R.; *Physics Letters A* , **2000**, *277*, 61.
    DOI: 10.1016/S0375-9601(00)00694-0
26. Darmanyan, S.; Nevière, M.; A. Zakhidov; *Optics Communications*, **2003**, *225*, 233.
    DOI: 10.1016/j.optcom.2003.07.047
27. Solymar., L.; Shamonina E.; *Waves in Metamaterials*, Oxford University Press, UK, **2009**.
    ISBN: 19780199215331

.

